Temperature evolution of Raman spectra and nature of phase transitions in $CuInP_2S_6$ and $Ag_{0.1}Cu_{0.9}InP_2S_6$ crystals

Kohutych A., Medulych M., Hryts V., Liubachko V., Vysochanskii Yu.

Institute for Solid State Physics and Chemistry, Uzhhorod National University, Uzhhorod, Ukraine

Introduction

Quaternary phosphorus chalcogenide $CuInP_2S_6$ represents a family of layered materials down to the nanoscale that exhibit intriguing properties related to ferrielectricity and accompanied by ionic conductivity [1]. The $CuInP_2S_6$ structure consists of lamellae defined by a sulphur framework in which the metal cations and P–P atomic pairs fill the octahedral voids; within a layer, Cu, In, and P–P form triangular patterns (Figure 1). At the first order phase transition that occurs at $T_c \sim 312$ K, there is a decrease in the space symmetry group from C2/c in the paraelectric phase to Cc in the ferrielectric phase due to the ordering of the Cu^+ cations in a polar sublattice, together with an opposite displacement of the In^{3+} ions, forming the second polar sublattice [2]. Both ions are displaced normally to the structural layers plane. As the off-centering of the Cu ions is much greater than that of In, the result is an uncompensated two-dimensional ferrielectric arrangement with total polarization perpendicular to the plane of the layers [1-2]. That cation off-centering is attributed to a second-order Jahn–Teller effect (SOJT), associated with the d^{10} electronic configuration of Cu^+ cations [2]. The thermal activation of Cu^+ cations in the local double-well potential associated with the SOJT also contributes to the increase in ionic conductivity in $CuInP_2S_6$ crystals upon heating to the temperature of the ferrielectric to paraelectric phase transition and in the paraelectric phase. The In^{3+} cations in the local three-well potential also play an important role in the mechanism and the character of dipole ordering in $CuInP_2S_6$-type ferrielectrics.

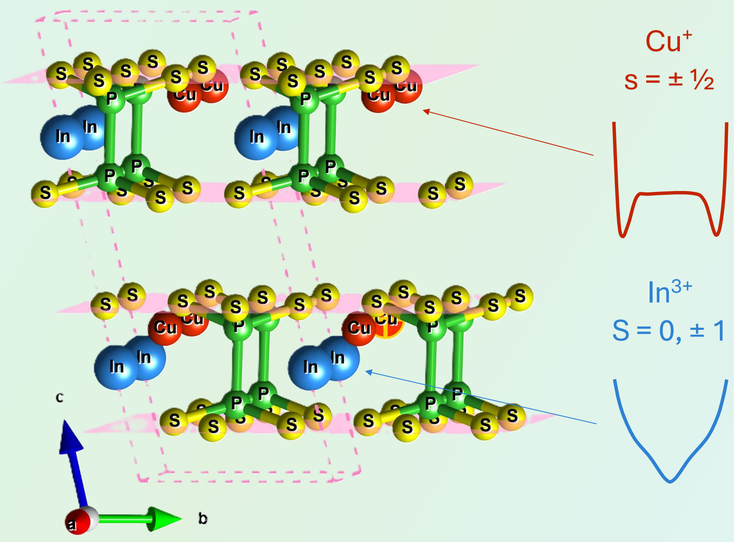

Figure 1. Layered $CuInP_2S_6$ crystal with four unit cells.

Experimental setup

The phenomenon of Raman light scattering was investigated utilizing a double grating spectral photometer (DFS24), wherein two diffraction gratings (replicas) with a stroke count of 1200 per 1 mm, operating in the first order of diffraction, function as dispersing elements. The light receiver is a Hamamatsu H11890-01 photomultiplier tube, which is equipped with a photon counting capability. The sequence of instantaneous values of light flux intensity, averaged with a given time constant, is recorded by an electrical circuit and stored (Figure 2). A NeNe laser (model LGN215, 50 mW) operating in single mode with a wavelength of 0.6328 μm was employed for the excitation of Raman scattering. Raman spectra were analyzed with a resolution of up to 1 cm^{-1}. The relative error of the intensity measurement at the line maxima, as well as the distortion of the half-widths of their contours in relation to the true half-widths of the spectral lines, was no more than 1%. The Oxford Optistat DN-X cryostat was used to perform the temperature measurements (80 – 440 K).

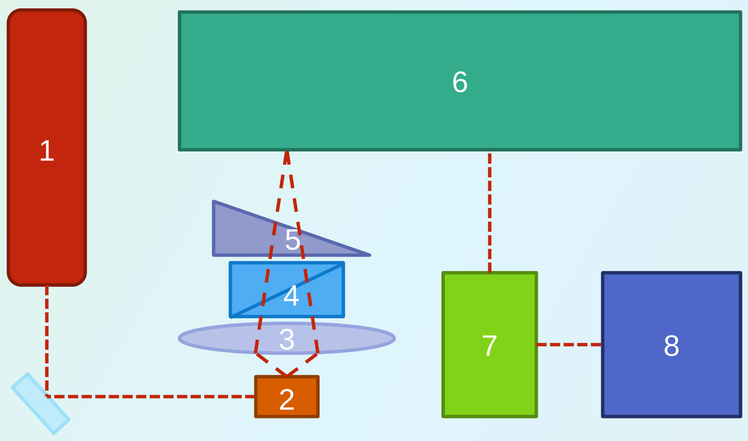

Figure 2. Experimental setup for the study of Raman light scattering spectra: 1 - HeNe laser; 2 - sample; 3 - condenser; 4 - analyzer; 5 - depolarizing wedge; 6 - DFS24 spectral photometer; 7 - registration system: photon counter Hamamatsu H11890-01; 8 - computer.

Raman scattering data of $CuInP_2S_6$ crystal

The Raman scattering data (Figures 3 and 4) obtained upon heating to 200 K revealed a softening of the Raman low-frequency spectral lines, which is related to the quantum fluctuations of the indium cationic sublattice. Above 200 K, the spectral lines exhibited broadening, which can be attributed to the disorder in the copper sublattice in the region with a classical character of thermal fluctuations.

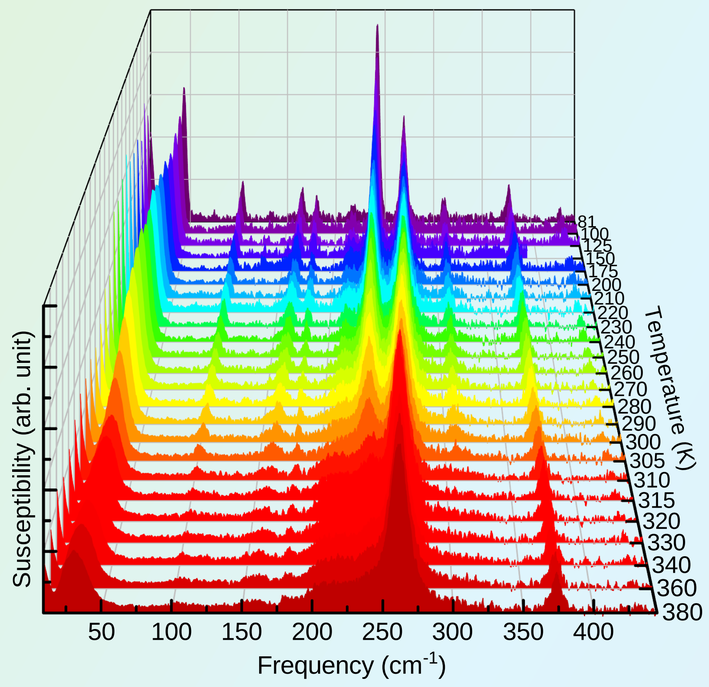

Figure 3. Temperature transformation of Raman spectra for $CuInP_2S_6$ crystal.

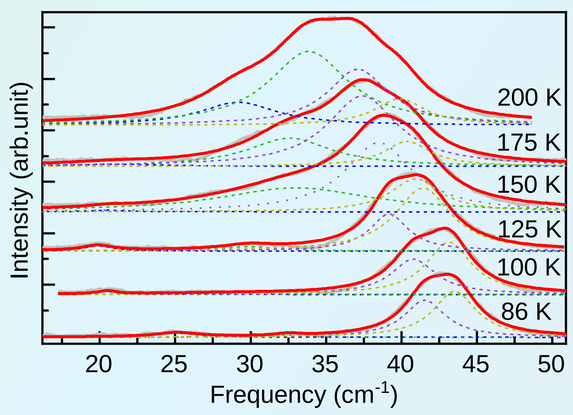

Figure 4. Low frequency Raman spectra for $CuInP_2S_6$ crystal at different temperatures.

The transition to the dipole glassy state in the Raman scattering (Figure 5) is illustrated through spectral peak intensity, width, and frequency changes with cooling from the temperature range of classical thermal fluctuations (red to green colored spectra) into the quantum fluctuations dominated interval (from blue to violet colored spectra). Spectroscopic data indicate that the coordination environments of the In^{3+} and Cu^+ cations undergo rearrangements, which can induce polar structural frustrations across the low temperature range of the ferrielectric phase.

Pressure transformation of Raman spectra

Uniaxial compression perpendicular to the structural layers increases the phase transition temperature due to the change in local potential, which is observed in the pressure-induced variation of the low-energy Raman spectral lines (Figure 6).

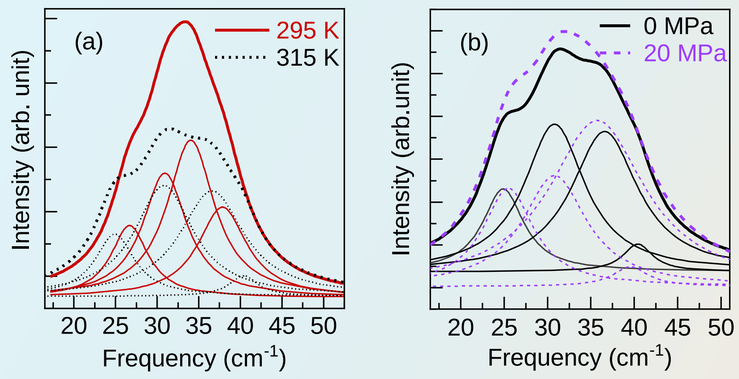

Figure 5. Low frequency Raman spectra for $CuInP_2S_6$ crystal at different temperatures (a) and under uniaxial pressure perpendicular to the structural layers at 315 K (b).

This feature is reflected in the negative sign of the electrostriction coefficients for the layered ferroelectric crystal $CuInP_2S_6$. The uniaxial pressure-induced change in the low-frequency Raman spectral lines is consistent with an increase in the temperature of the first order ferroelectric phase transition.

Partial substitution in the cationic sublattice

The transformation of the ferrielectric first order phase transition, which is observed for $CuInP_2S_6$, into the subsequent paraelectric to ferrielectric second order phase transition and the isostructural first order transition with a sharp change in the polarization in the ferrielectric phase was revealed for $Ag_{0.1}Cu_{0.9}InP_2S_6$ mixed crystal [3]. In the case of $Ag_{0.1}Cu_{0.9}InP_2S_6$, an additional Raman band at 250 cm^{-1} appears which is similar to that observed in the case of $AgInP_2S_6$ crystal (Figures 6) and corresponds to the lattice vibration resulting from the displacement of In^{3+} cations and the deformation of the anionic structural groups of $(P_2S_6)^{4-}$.

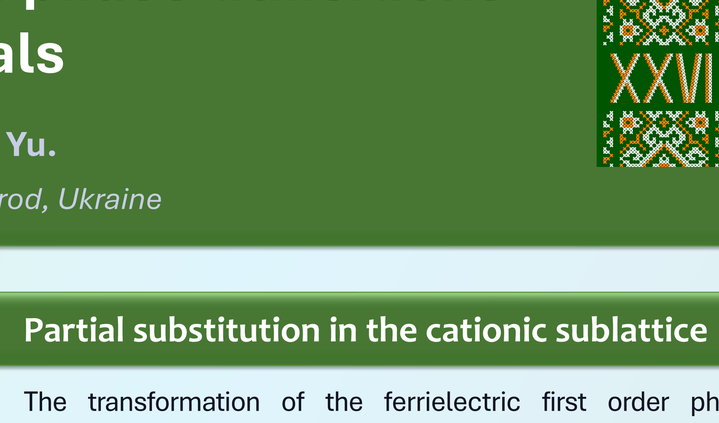

Figure 6. Calculated phonon dispersion branches and partial contributions of atoms to the energy distribution of the phonon density of states of $AgInP_2S_6$ compound.

Below 200 K (Figure 7) a significant transformation of the spectra is observed, which is associated with the anharmonic dynamics of indium cations. When $Ag_{0.1}Cu_{0.9}InP_2S_6$ is heated from 200 K to 250 K, the Raman spectra are also drastically changed. This is related to the change in shape of the three-well local potential of In^{3+} cations due to change in internal chemical pressure at partial substitution of copper by silver. The smearing of the spectra in the range of 270-295 K is related to a gradual decrease in the crystal structure spontaneous polarization during sequential phase transitions. In contrast to the Raman spectrum of the pure $CuInP_2S_6$ crystal, the $Ag_{0.1}Cu_{0.9}InP_2S_6$ spectrum continues to demonstrate notable temperature-dependent alterations when heated in the paraelectric phase.

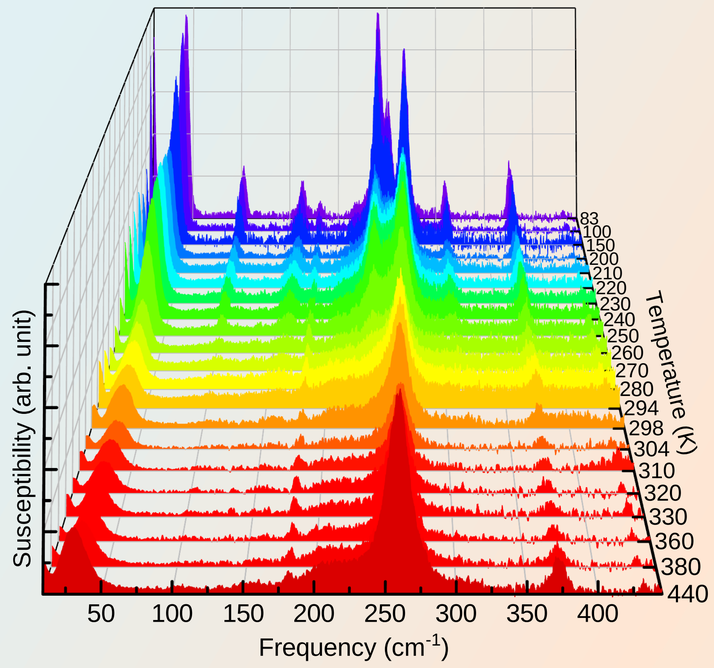

Figure 7. Temperature transformation of Raman spectra for $Ag_{0.1}Cu_{0.9}InP_2S_6$ crystal.

Conclusions

In this study, we have performed Raman spectroscopy experiments on $CuInP_2S_6$ and $Ag_{0.1}Cu_{0.9}InP_2S_6$ crystals across a wide temperature range (80-440 K). Furthermore, we have investigated the temperature-dependent evolution of the spectra under pressure, with the objective of elucidating the anharmonic lattice dynamics and the nature of phase transitions in these van der Waals crystals. The results of this study revealed significant temperature-dependent changes in the Raman spectra when copper was partially substituted by silver in the cation sublattice or under the influence of uniaxial pressure. The obtained Raman spectra were analyzed with the DFT-calculated phonon spectra data for $CuInP_2S_6$ and $AgInP_2S_6$ crystals as well as with simulations in a four-well quantum anharmonic oscillator model, which characterizes the anharmonic dynamics of the copper and indium sublattices in $CuInP_2S_6$ crystals.

References

1. J. Banys, A. Dziaugus, K. Glukhov, A. Morozovska, N. Morozovsky, Yu. Vysochanskii, Van der Waals Ferroelectrics. Properties and Device Applications of Phosphorous Chalcogenides, Willey-VCH, 2022, 381 p.

2. V. Maisonneuve, V. B. Cajipe, A. Simon, R. Von Der Muhll, and J. Ravez, Phys. Rev. B, 1997, doi: 10.1103/PhysRevB.56.10860

3. T. Babuka, K. Glukhov, Yu. Vysochanskii, M. Makowska-Janusik, RSC Advanced, 2018, doi: 10.1039/C7RA13519J.